The Scientific Journal of King Faisal University

Basic and Applied Sciences

Impact of Solvents, Magnesium Oxide and Aluminium Oxide Nanoparticles on the Photophysical Properties of Acridine Orange Dye

Fairooz Faeq Kareem, Mahasin F. Hadi Al-Kadhemy and Asrar Abdulmunem Saeed

Department of Physics, College of Science, Mustansiriyah University, Baghdad, Iraq

LINK	RECEIVED	ACCEPTED	PUBLISHED ONLINE	ASSIGNED TO AN ISSUE
https://doi.org/10.37575/b/sci/210047	18/08/2021	26/11/2021	26/11/2021	01/12/2021
NO. OF WORDS	**NO. OF PAGES**	**YEAR**	**VOLUME**	**ISSUE**
5495	7	2021	22	2

ABSTRACT

Absorption and fluorescence spectroscopy techniques were applied to investigate the photophysical characteristics of acridine orange (AO) dye in solvents that included distilled water, dimethyl sulfoxide (DMSO), acetone and ethanol in various concentrations (1×10-4—1×10-6) M. All of the samples were served at room temperature. The relationships between various parameters describing the strength of optical transitions in atoms and molecules were reviewed. This study expresses various viewpoints by describing how concentration and solvent affect the dye's absorption and fluorescence spectra. The absorption spectra of AO exhibit a band at (490 nm), except for DMSO, which shifts more towards red by 5 nm. The fluorescence spectra show a blue shift in AO aqueous solution around 6 nm until (0.5×10-4) M, followed by a red shift at around 7 nm at (1×10-6) M. There is a blue shift in (1×10-5) M for DMSO at around 4 nm, then a 10 nm red shift in higher concentrations as well as a 9 nm red shift in acetone and 6 nm in ethanol. Adding magnesium oxide nanoparticles (MgO NPs) quenched AO in both absorption and fluorescence spectra, whereas maximum fluorescence and intensity increased when aluminium oxide nanoparticles (Al2O3 NPs) were added to the solution.

KEYWORDS

Laser dye, absorption spectrum, fluorescence spectrum, MgO NPs, Al2O3 NPs

CITATION

Kareem, F. F., M. F. H. Al-Kadhemy, and A. A. Saeed. (2021). Impact of solvents, magnesium oxide and aluminium oxide nanoparticles on the photophysical properties of acridine orange dye. *The Scientific Journal of King Faisal University: Basic and Applied Sciences*, **22**(2), 113–9. DOI: 10.37575/b/sci/210047

1. Introduction

Acridine is a cationic dye that shares a common aromatic structure with multiple acridine dyes (Sharma *et al.* 2003). Acridine has various applications in fluorescence microscopy, endomicroscopy, intraoperative, fluorescence guidance, photodynamic therapy, sonodynamic therapy and radio dynamic therapy (Byvaltsev *et al.* 2019).

Acridine derivatives form an important class of heterocycles containing nitrogen due to their broad range of pharmaceutical properties. In the nineteenth century, acridine derivatives were used industrially as pigments and dyes. More critical to the pharmaceutical industry, acridines are used as dyes, fluorescent materials for visualisation of biomolecules and in laser technologies. The properties of acridines are attributed to their semi-planar heterocyclic structure, which appreciably interacts with different biomolecular targets. Acridine/acridone derivatives are found in natural plants and various marine organisms (Kowalewska *et al.* 2017).

The $S_0 \longrightarrow S_1$ and $S_0 \longrightarrow S_2$ bands in acridine orange (AO) are red shifted in polar solvents compared to non-polar solvents, indicating that the transitions are $\pi \rightarrow \pi^*$ in nature. The ground state has a higher charge character than the excited state. In contrast, the $S_0 \longrightarrow S_3$ bands are blue-shifted in polar compared to non-polar solvents (Sikiru *et al.* 2016).

Nanomaterials, particularly metal and metal oxide nanoparticles, are a special class of materials with unique physical and chemical properties that have a wide range of applications. Magnesium oxide nanoparticles (MgO NPs) have been used in electronics, catalysis, additives, ceramics, photochemical products, paints and medicine (Musarat *et al.* 2020). Engineered aluminium oxide nanoparticles (Al_2O_3 NPs) have commercial potential in catalysis, polymer modification and heat transfer fluids (Sunandan *et al.* 2013). Kumar *et al.* (2018) investigated the use of MgO as the adsorbent for methylene blue (MB) removal. It is also possible to extract spectral information from the adsorbed compounds using nanoporous aluminium oxide, as demonstrated by Hotta *et al.* (2010).

Absorption and fluorescence spectra reveal significant changes due to aggregations, which can be useful as the parameters change when the concentration of AO decreases. This study aims to characterise AO's absorption and fluorescence properties as a function of its concentration by calculating the quantum yield, extinction coefficient, Stokes shift, radiative lifetime and fluorescence lifetime. As AO is used in medical applications and MgO and Al_2O_3 are used in industrial applications at low cost, metal oxide nanoparticles were added to the AO water solution and studied as a new work.

2. Experimental Work

2.1 Materials:

AO ($C_{17}H_{19}N_3.1/2ZnCl_2.HCl$, molecular weight 369.94 g/mol) from Qualikems Fine Chem Pvt. Ltd. was dissolved in distilled water, dimethyl sulfoxide (DMSO), acetone and ethanol. Distilled water (H_2O) with (10.2) polarity and DMSO (C_2H_6OS) with (7.2) polarity (Lide, 2010) were procured from Greyhound Chromatography and Allied Chemicals. Acetone (CH_3COCH_3) with (5.1) polarity (Lide, 2010) was acquired from HI Media Laboratories Pvt. Ltd, and ethanol (C_2H_5OH) with (4.0) polarity (Lide, 2010) was procured from Finchley, London. The solvents were supplied with 99% purity in terms of mass percentage.

Magnesium oxide (MgO with an average diameter of 40 nm and 99.9% purity) was obtained from Intelligent Materials Pvt. Ltd. Alumina oxide (Al_2O_3 with an average diameter of 20—30 nm and 99.9% purity) was obtained from China.

2.2 Preparation of Samples:

AO dye solution with a primary concentration of (1×10^{-2}) M was prepared by dissolving appropriate amounts of dye (weighted by a Mattler balance of 0.1 mg sensitivity) in the solvents. The amount of dye, m (in g), was calculated using equation (1) (Al-Kadhemy *et al.* 2020):

Corresponding Author: Fairooz Faeq Kareem 009647703467140, cenderlla78@yahoo.com

$$m = \frac{M_W V C}{1000} \quad (1)$$

where M_w is the molecular weight of dye (g/mole), V is the volume of the solvent (ml) and C is the dye concentration (M), which was then diluted to get concentrations in the range of (1×10^{-2}) M to (1×10^{-6}) M as shown in equation (2) (Krolenko *et al.* 2006; Saeed *et al.* 2020).

$$C_1 V_1 = C_2 V_2 \quad (2)$$

where C_1 is high concentration, V_1 is the volume before dilution, C_2 is low concentration and V_2 is the total volume after dilution. It was noted that the prepared solutions had good homogeneity.

Nano (MgO and Al_2O_3) was added to the dye solution in 0.002 g and 0.004 g amounts. The mixture for both nanomaterials was added to the dye solution to investigate the best number of nanoparticles to enhance the photophysical properties of the organic dye. All of the samples were prepared using a hot plate magnetic stirrer until the (MgO and Al_2O_3) nanoparticles were diffused homogeneously through the AO distilled water solution. All of the samples were kept in a dark place to avoid any possibility of photo-bleaching or the dye fading. The samples were used immediately after preparation.

Spectrophotometric measurements were taken with a UV-Visible spectrophotometer (T70/T80) and (SHIMADZU RF-5301pc) for absorption and fluorescence spectra for all samples, respectively. All of the figures were created with Origin Pro 2019b.

3. Theory and Calculations

The intensity of light absorption at wavelength λ by an absorbing medium is characterised by absorbance A (λ) or transmittance T (λ), defined as (Valeur 2012):

$$A(\lambda) = log\frac{I_o}{I} = -\log(\lambda) \quad (3)$$

where I_o and I are the light intensities of the beams entering and leaving the absorbing medium, respectively. In many cases, the absorbance of a sample follows the Beer–Lambert Law (Valeur 2012).

$$A(\lambda) = \log\frac{I_o}{I} = \varepsilon(\lambda) l C \quad (4)$$

where $\varepsilon(\lambda)$ is the molar absorption coefficient that represents a molecule's ability to absorb light in a given solvent (commonly expressed in L mol^{-1} cm^{-1}), C is the concentration (in M) of the absorbing species and L is the absorption path length (thickness of the absorbing medium in cm). According to classical theory, molecular absorption of light can be described by considering the molecule as an oscillating dipole, which allows us to introduce a quantity called the oscillator strength (*f*), which is directly related to the integral of the absorption band as follows (Dihingia *et al.* 2019):

$$f = 2303\ \frac{mC_o^2}{N_a\ \pi e^2\ n} \int \varepsilon(\bar{\nu}) d\bar{\nu} \quad (5)$$

where m and e are the mass and charge of an electron, respectively, Co is the speed of light, n is the index of refraction and $\overline{\nu}$ is the wavenumber (in cm^{-1}). Oscillator strength, *f*, is a ratio that compares the strength of the transition with that of a bound electron behaving as a 3D harmonic oscillator. For strong molecular transitions, *f* values are close to 1 (sometimes they even slightly exceed this value). For weak transitions, *f* values can be several orders of magnitude lower than 1 and as low as 10^{-8}. For $n \longrightarrow \pi^*$ transitions, the values of ε are in the order of a few hundred or less and those of *f* are no greater than $\sim10^{-3}$. For $\pi \longrightarrow \pi^*$ transitions, the values of ε and *f* are, in principle, much higher (except in symmetry-forbidden transitions); *f* is close to 1 for some compounds, which corresponds to values of ε that are of the order of 10^5. *f* is a dimensionless quantity (Birks 1973).

Fluorescence quantum yield (Φ_F) is the ratio of the number of emitted photons (over the entire duration of decay) to the number of absorbed photons (Valeur 2012).

$$\Phi_F = \frac{\text{number of photons emitted}}{\text{number of photons absorbed}} = \frac{\int Area\ under\ the\ fluoresence\ spectrum}{\int Area\ under\ the\ absorption\ spectrum} \quad (6)$$

where the number of photons emitted and absorbed are in the integrated area under the fluorescence and absorption spectrum, respectively.

Radiative lifetime (τ_{FM}) has been related to the extinction coefficient using a variety of formulas. Bowen and Woks' method is the easiest to utilise (Valeur 2012):

$$\frac{1}{\tau_{FM}} = 2.88 \times 10^{-9} n^2 \bar{\nu}^2 \int \varepsilon(\bar{\nu}) d\bar{\nu} \quad (7)$$

where ($\int \varepsilon\ (\bar{\nu})\ d\bar{\nu}$) is the area under the curve of the molecular extinction coefficient plotted against the wavenumber, $\bar{\nu}$ is the wavenumber of the maximum in the absorption band and n is the refractive index of the solvent.

Then, fluorescence lifetime (τ_F) is obtained using the following equation (Valeur 2012):

$$\tau_F = \phi_F \tau_{FM} \quad (8)$$

Stokes shift ($\Delta\bar{\nu}$) is the term used to describe the difference in the wavelength at which a molecule emits light and is relative to the wavelength at which the molecule was excited (Al-Kadhemy and Nasser 2018).

$$\Delta\bar{\nu} = \bar{\nu}_{abs.} - \bar{\nu}_{flu.} \quad (9)$$

This important parameter can provide information about excited states. For instance, when the dipole moment of a fluorescent molecule is higher in an excited state than in a ground state, the Stokes shift increases with solvent polarity (Takashi *et al.* 2010).

The full width at half maximum (FWHM) is calculated by knowing the half intensity of absorption or fluorescence spectra that determines the half-width of spectra by slipping towards the x-axis, which represents the wavelength in nanometres (Lewkowics 2006). The FWHM is the function of the possibility of tunability in the active medium laser.

4. Results and Discussion

The absorption spectra of AO laser dye in different solvents (distilled water, DMSO, acetone and ethanol) at various concentrations (1×10^{-4}, 0.5×10^{-4}, 1×10^{-5}, 0.5×10^{-5} and 1×10^{-6}) M is illustrated in Figure (1). The maximum excitation and emission (λ_{max}) for standard AO (in aqueous solution) is (494 nm) and (525 nm), respectively (Krolenko *et al.* 2006).

Figure (1a) shows AO dissolved in distilled water. It is a noticeably wide spectrum with the maximum absorption wavelength constant at all concentrations at 490 nm and around 470 nm at the shoulder. This is consistent with Krolenko *et al.* (2006). The intensity of absorption increases as the concentration increases. A further increase in concentration leads to a decrease in the absorption band at 490 nm, and the shoulder increases at 470 nm, which can be assigned to the dimer and monomer (Falcone *et al.* 2002; Markarian and Gohar 2015).

This can be observed in Figure (1b) where AO is dissolved in DMSO, which is less polar than distilled water. The same behaviour is noticed for maximum absorption wavelength, which is unchangeable with increasing concentrations, but a red shift occurs and becomes 495 nm compared to the water solvent. Absorption intensity increases with increasing concentration, which is in agreement with Markarian and Gohar (2015). In both of the solvents mentioned above, the FWHM decreases with increasing concentration, and the spectra become narrower. The physical and chemical characteristics of DMSO are unique, and it has a higher polarity than both ethanol and acetone. It has a high dielectric constant, making charge separation simple, and it is soluble in a wide range of ionic, polar and polarisable molecules.

DMSO is also a good solvent for olefin polymerisation because its hydrogen atoms are resistant to being removed in free-radical processes. DMSO solvates cations, in general, due to the increased electron density of the oxygen atom and the steric availability of oxygen. The basicity of DMSO is somewhat higher than that of water because of the increased electron density near the oxygen atom. DMSO's capacity to compete successfully for hydrogen donor molecules is a key element in its influence on various reaction speeds. As the reactivity of bases in DMSO increases, a variety of base-catalysed elimination and cleavage processes can be carried out at room temperature or temperatures much lower than normal.

Acetone (Figure (1c)) and ethanol (Figure (1d)) have lower polarity than water; therefore, the maximum absorption wavelength does not change with increased concentrations of AO and remains at 490 nm with the smaller shoulder at 470 nm. Absorbance increases regularly with increasing concentration due to an increase in the number of excited AO molecules from a ground state to the first excited state, which aligns with Al Hussainey *et al.* (2018). For both solvents, the FWHM of absorption spectra (increase in acetone and decrease in ethanol) increases the concentrations. Table (1) displays all of the results that are discussed above.

Comparing the absorbance results for all of the previous solvents shows that the maximum wavelength of absorption spectrum remains constant, except for DMSO, which shifts more towards red by 5 nm. Absorbance increases with the increasing polarity of the solvent and has the highest absorbance for water with higher polarity.

Figure (1): Absorption spectra of AO in a) distilled water; b) DMSO; c) acetone; d) ethanol in various concentrations

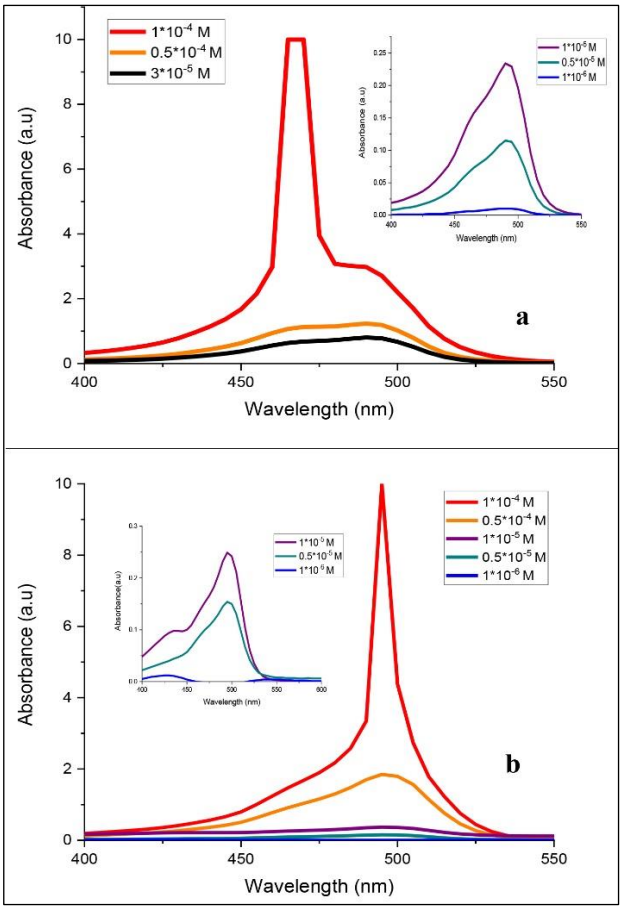

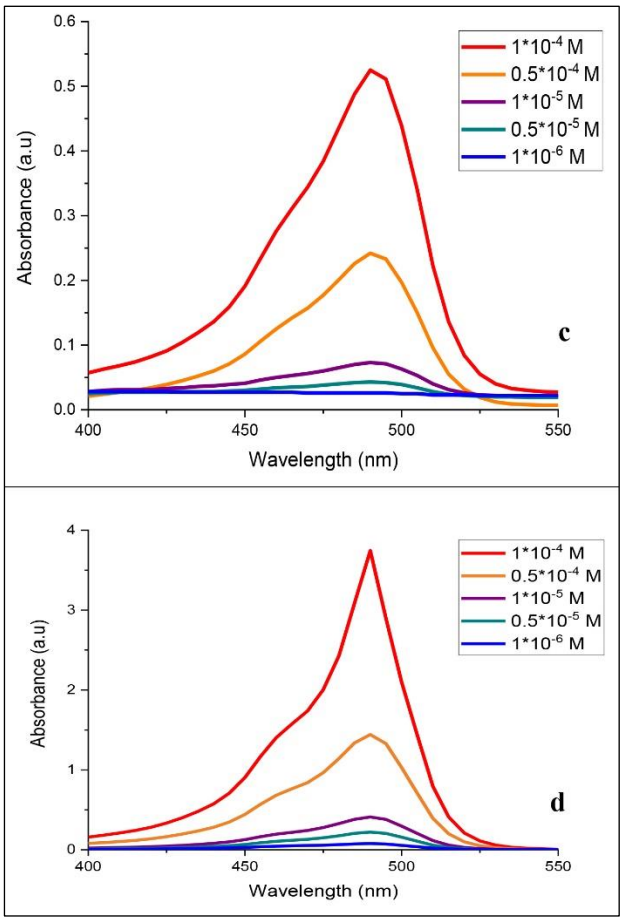

Table (1): Absorption parameters for AO in different solvents with different concentrations

Solvents	C (M)	λ_{absmax} (nm)	$I_{abs\ max}$	FWHM (nm)
Distilled water	1×10^{-4}	490	2.98	12.68
	0.5×10^{-4}	490	1.23	58.81
	1×10^{-5}	490	0.23	52.93
	0.5×10^{-5}	490	0.11	51.53
	1×10^{-6}	490	0.01	56.66
	3×10^{-5}	490	0.80	56.67
DMSO	1×10^{-4}	495	2.88	8.20
	0.5×10^{-4}	495	1.84	44.57
	1×10^{-5}	495	0.24	53.93
	0.5×10^{-5}	495	0.15	55.58
	1×10^{-6}	490	0.07	155.84
Acetone	1×10^{-4}	490	0.52	53.55
	0.5×10^{-4}	490	0.24	57.50
	1×10^{-5}	490	0.07	210
	0.5×10^{-5}	490	0.04	170
	1×10^{-6}	490	0.04	35
Ethanol	1×10^{-4}	490	3.75	29.30
	0.5×10^{-4}	490	1.44	42.64
	1×10^{-5}	490	0.41	43.99
	0.5×10^{-5}	490	0.23	44.95
	1×10^{-6}	490	0.08	51.67

As a result of fast internal conversion from higher initial excited states to the lowest vibrational energy level of an excited state, the emission spectrum is independent of excitation energy (wavelength). The vibrational energy level spacing in the ground and excited states of many common dyes is similar, leading to a fluorescence spectrum that strongly matches the absorption spectrum. This is because the most optimal transitions of absorption and fluorescence are the same. Figure (2) shows the fluorescence spectra of AO laser dye in different solvents (distilled water, DMSO, acetone and ethanol) at various concentrations (1×10^{-4}, 0.5×10^{-4}, 1×10^{-5}, 0.5×10^{-5}, 1×10^{-6}) M. The detailed vibrational structure is usually lost, and the fluorescence spectrum behaves as a broad band.

Figure (2a), which is related to the fluorescence spectra of AO dissolved in distilled water, shows the effects of increasing the fluorescence intensity with increasing concentration until aggregation occurs at (1×10^{-4}) M. The maximum fluorescence

wavelength decreases when the concentration increases from 1×10^{-6} M to 0.5×10^{-4} M (blue shift about 7 nm), then the red shift is obtained (about 6 nm) for 1×10^{-4}M.

Figure (2b), where AO is dissolved in DMSO, shows the effects of decreasing the maximum fluorescence wavelength while increasing the concentration; a blue shift occurs around 4 nm for 1×10^{-5}M, then a red shift is shown for the higher concentration of 10 nm. The fluorescence intensity increases with increased concentration, except for 1×10^{-4} M, where it decreased due to dye aggregation.

For AO dissolved in acetone (Figure (2c)), a red shift can be noted (towards a long wavelength) at around 9 nm as fluorescence intensity increases when the concentration is increased.

The maximum wavelength of fluorescence spectra of AO dissolved in ethanol, as shown in Figure (2d), directly increases with concentration and obtains a 6 nm red shift. Fluorescence intensity increased until 1×10^{-4} M, then decreased as a result of the formation of dye aggregation. Inner filter effects and aggregation can reduce the fluorescence intensity when fluorescent dye concentrations are high. As seen from the fluorescence results of increasing acridine concentration, photons generated at wavelengths corresponding to the intersection between the absorption and emission spectra may be reabsorbed (auto-absorption by solution), as shown in research by Al-Kadhemy and Nasser (2018) (Albani 2007). For all solvents, the FWHM of fluorescence spectra decreased when concentration increased, as shown in Table (2).

Figure (2): Fluorescence spectra of AO in a) distilled water; b) DMSO; c) acetone; d) ethanol in various concentrations

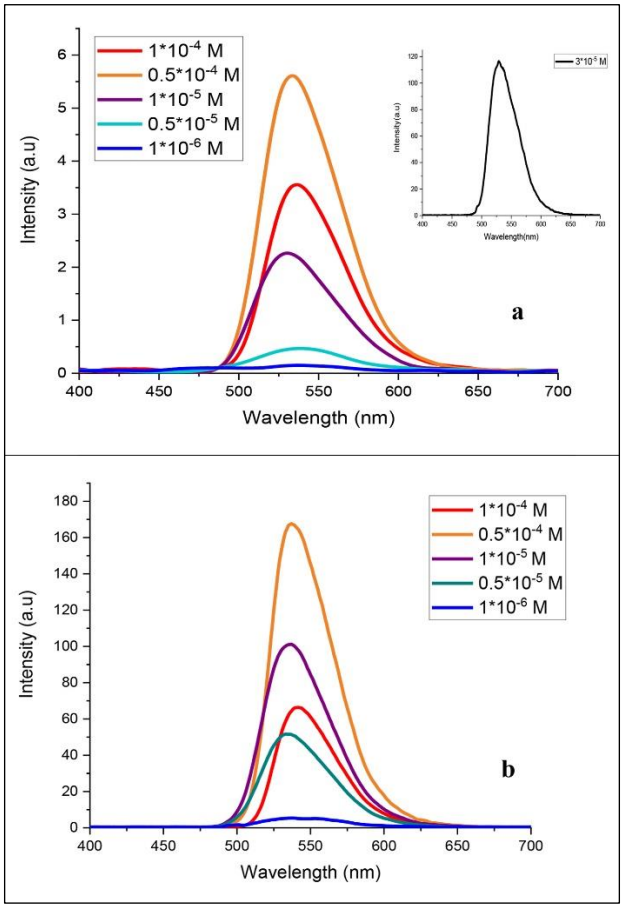

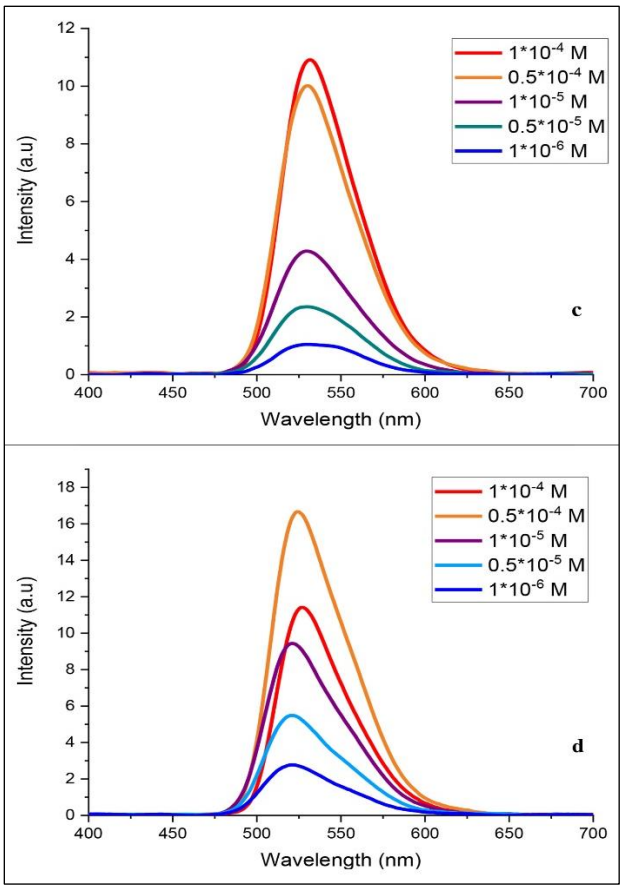

Table (2): Fluorescence parameters for AO in different solvents with different concentrations

Solvents	C (M)	$\lambda_{fluo.max}$ (nm)	$I_{fluo.\ max.}$	FWHM (nm)
Distilled water	1×10^{-4}	536	3.85	55.58
	0.5×10^{-4}	533	5.60	56.74
	1×10^{-5}	530	2.33	60.84
	0.5×10^{-5}	539	0.47	67.98
	1×10^{-6}	537	0.18	86.27
	3×10^{-5}	529	117.19	22.66
DMSO	1×10^{-4}	540	0.40	16.17
	0.5×10^{-4}	536	1.00	20.22
	1×10^{-5}	530	0.59	15.33
	0.5×10^{-5}	535	0.30	24.08
	1×10^{-6}	534	0.32	19.74
Acetone	1×10^{-4}	530	1.01	21
	0.5×10^{-4}	529	0.93	50.39
	1×10^{-5}	527	0.41	18.09
	0.5×10^{-5}	521	0.22	14.18
	1×10^{-6}	521	0.12	5
Ethanol	1×10^{-4}	527	11.4	48.01
	0.5×10^{-4}	524	16.6	52.27
	1×10^{-5}	521	9.4	53.08
	0.5×10^{-5}	520	5.5	53.4
	1×10^{-6}	521	2.7	54.6

The oscillator strength (f) counts how much of the total oscillating potential is used for a specific transition. It was calculated from equation (5), with all of the f results less than 1, so the type of transition is $\pi \longrightarrow \pi^*$, as shown in Table (3).

As the energy required for fluorescence emission transitions (see Figs. (2, 3)) often becomes less than that associated with absorption, the emitted photons tend to have less energy and are shifted to higher wavelengths as a result. Stokes shift is a phenomenon that affects almost all dyes in a solution. The quick decay of excited electrons to the lowest vibrational energy level of the first excited state is the fundamental cause of Stokes shift. Fluorescence emission is also influenced by transitions to higher vibrational energy levels of the ground state, resulting in additional excitation energy loss caused by thermal equilibration of extra vibrational energy.

AO is a cationic dye that is protonated at a pH lower than 10, even in aqueous-only solutions. An important property of acridine is that its spectrum does not agree with Beer–Lambert law (as shown in DMSO

and distilled water) due to molecular aggregation as a result of strong dipole–dipole interaction in aggregate units. It should be noted that the aggregates, particularly dimers compared to monomers, show different photophysical and spectroscopic properties. In general, the photophysical and spectroscopic properties of dye molecules depend upon the aggregation type. There are numerous spectroscopic studies regarding self-association and protonation of acridine in aqueous solutions. This result is in agreement with Falcone *et al.* (2006) and Robinson *et al.* (1972).

To illustrate the overlap between absorption and fluorescence spectra, the best concentration of acridine dissolved in distilled water was (3×10^{-5}) M, as shown in Figure (3a). The maximum absorption wavelength (λ_{abs}) was 490 nm, and the fluorescence wavelength (λ_{fluo}) was 529 nm. Figure (3b) displays the best concentration of AO dissolved in DMSO at (1×10^{-5}) M, which obeys Beer–Lambert law. The maximum absorption wavelength (λ_{abs}) was 490 nm, and the fluorescence wavelength (λ_{fluo}) was 521 nm.

The best concentration of AO dissolved in acetone was (1×10^{-5}) M, which obeys Beer–Lambert law. The maximum absorption wavelength (λ_{abs}) was 495 nm, and the fluorescence wavelength (λ_{fluo}) was 530 nm, as shown in Figure (3c). Figure (3d) displays the best concentration of AO dissolved in ethanol at (1×10^{-5}) M, which obeys Beer–Lambert law. The maximum absorption wavelength (λ_{abs}) was 490 nm, and the fluorescence wavelength (λ_{fluo}) was 521 nm.

Figure (3) demonstrates that Stokes shift increases when the concentrations in all acridine dye solutions are increased (except the acridine water solution), as seen in Table (3). Additionally, the fluorescence spectrum is typically a mirror image of the absorption spectrum resulting from the ground to the first excited state transition. Furthermore, all peaks are symmetric.

The magnitude of Stokes shift is influenced by the dye and its solvation environment. It is measured from equation (9), with greater Stokes shifts appearing in more polar solvents. As seen in Figure (3) and the data in Table (3), Stokes shift is highest in water (more polar) and lowest in ethanol (less polar). Stokes shift is necessary for fluorescence imaging measurements to have such great sensitivity, and because of the red emission shift, precise bandwidth optical filters can effectively stop excitation light from reaching the detector, allowing the relatively faint fluorescence signal (with a small number of released photons) to be detected against a low-noise background.

Figure (3): Absorption and fluorescence spectra of AO in a) distilled water; b) DMSO; c) acetone; d) ethanol at the best concentration

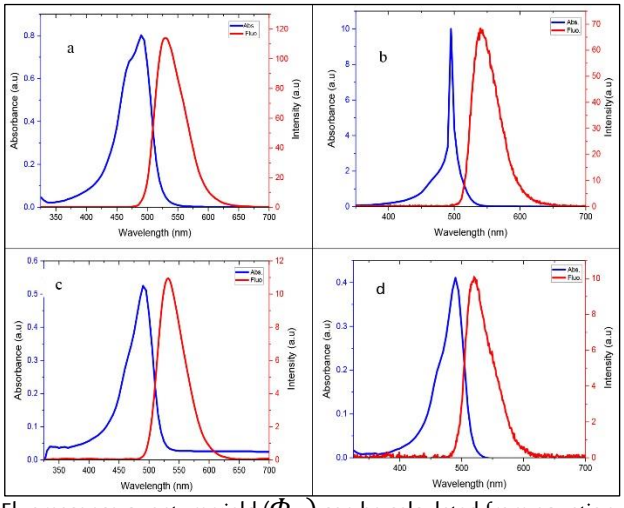

Fluorescence quantum yield (Φ_F) can be calculated from equation (6) for all solvents, as shown in Table (3). The best value is (0.97) in distilled water at a concentration of (0.5×10^{-4}) M. Their values did not exceed 1 and varied with changing concentrations and solvents for the AO dye. For the absorption spectra of all samples, the radiative lifetime (τ_{FM}) is calculated from equation (7). Generally, the maximum value is (55.5) ns for a concentration of (1×10^{-4}) M in DMSO. Their values differ according to concentrations and solvents. From these two parameters and as stated by equation (8), the fluorescence lifetime (τ_F) is planned, as seen in Table (3). The best value is in acetone, especially at the concentration of (0.5×10^{-4}) M, resulting in (13.5) ns.

Table (3): Photophysical parameters for AO in different solvents with different concentrations

Solvents	C (M)	Stokes shift (nm)	f	Φ_F	τ_{FM} (ns)	τ_F (ns)
Distilled water	1×10^{-4}	46	0.37	0.45	3.7	1.6
	0.5×10^{-4}	43	0.24	0.97	6.1	5.9
	1×10^{-5}	40	0.20	0.43	7.4	3.1
	0.5×10^{-5}	49	0.19	0.86	7.7	6.6
	1×10^{-6}	47	0.09	0.42	5.41	2.2
	3×10^{-5}	39	0.25	0.54	5.94	3.2
DMSO	1×10^{-4}	45	0.02	0.03	55.5	1.6
	0.5×10^{-4}	41	0.03	0.28	33.5	9.3
	1×10^{-5}	35	0.11	0.18	9.6	1.7
	0.5×10^{-5}	40	0.05	0.14	19.9	2.7
	1×10^{-6}	44	0.14	0.005	7.7	0.03
Acetone	1×10^{-4}	40	0.08	0.38	17.1	6.4
	0.5×10^{-4}	39	0.09	0.89	15.2	13.5
	1×10^{-5}	37	0.24	0.51	5.9	3.00
	0.5×10^{-5}	31	0.56	0.26	2.5	0.65
	1×10^{-6}	31	0.56	0.35	1.3	0.45
Ethanol	1×10^{-4}	37	0.17	0.08	7.9	0.6
	0.5×10^{-4}	34	0.19	0.23	7.2	1.6
	1×10^{-5}	31	0.30	0.44	4.6	2.02
	0.5×10^{-5}	30	0.34	0.45	4.0	1.8
	1×10^{-6}	31	0.84	0.49	1.6	0.7

The best concentration of AO dissolved in distilled water that obeys Beer–Lambert law is (3×10^{-5}) M mixed with (MgO and Al_2O_3) nanoparticles. To study the effect of these NPs on acridine dye solution, Figure (4) displays the absorption spectra of AO with different amounts of (MgO and Al_2O_3) nanoparticles. The maximum absorption wavelength (λ_{abs}) for AO in an aqueous solution is 490 nm with 0.80 maximum intensity. When MgO NPs are added to AO, the intensity decreases to 0.58, which may be related to MgO's ability to adsorb AO. The intensity of adding Al_2O_3 NPs to AO is 0.94, which raises the spectrum. The intensity of mixed (MgO and Al_2O_3) nanoparticles is 0.65, which also decreases the absorption spectrum. The maximum absorption wavelength (λ_{abs}) is 490 nm in all samples of NPs/AO aqueous dye solution.

Fig. (4): Absorption spectra of AO with (0.004 and 0.002) g of (MgO and Al_2O_3) nanoparticles

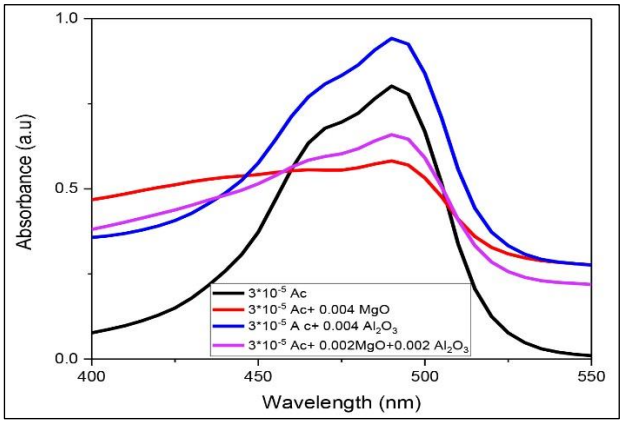

Figure (5) displays the fluorescence spectra of AO with different amounts of (MgO and Al_2O_3) nanoparticles. The maximum wavelength for AO in an aqueous solution is 529 nm with 117.19 maximum intensity. Maximum fluorescence wavelength and intensity both decreased when MgO NPs were added to AO. There was a noticeable increase in maximum fluorescence wavelength and intensity when Al_2O_3 NPs were added. Finally, adding the (MgO and Al_2O_3) mixture to the AO dye solution resulted in an increase in the maximum fluorescence wavelength and decreased intensity, as seen

in Table (4).

Fig. (5): Fluorescence spectra of AO with (0.004 and 0.002) g of (MgO and Al_2O_3) nanoparticles

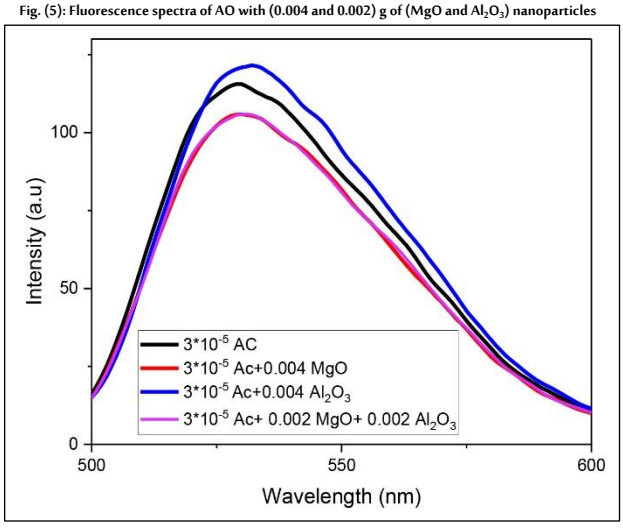

Table (4) shows that adding MgO decreased the absorption and fluorescence spectra intensity as well as the maximum wavelength.

Table (4) also displays an increase in both the maximum wavelength and intensity for absorption and fluorescence spectra. The result demonstrates that MgO NPs quench AO in both absorption and fluorescence spectra, and increase the maximum fluorescence and intensity when adding Al_2O_3 NPs to the solution. It is clear that the absorption spectra increased with the increased particle size of NPs. Al is a metal; therefore, it may generate electrons and transform into a cation. Al_2O_3 NPs may also absorb water, making them useful as a drying agent. Due to its great stability, it is also considered an oxidising agent.

Stokes shift in AO aqueous solution is best at a concentration of 39 (see Table 3). When MgO is added to the AO aqueous solution, Stokes shift decreases to 37. Adding Al_2O_3 enhances the Stokes shift, and it becomes 41 in both the Al_2O_3 AO aqueous solution and a mix of MgO and Al_2O_3 AO aqueous solution. This result leads to a rise in fluorescent molecules in an excited state.

Table (4): Spectral information for (MgO and Al_2O_3) – AO aqueous dye solution

AO in distilled water (3×10^{-5}) M	Amount of MgO NPs (g)	Amount of Al_2O_3 NPs (g)	λabs max (nm)	Labs	λfluo max (nm)	Ifluo	Stokes shift (nm)
	0.004	0	490	0.58	527	105.97	37
	0	0.004	490	0.73	531	123.67	41
	0.002	0.002	490	0.65	531	106.87	41

5. Conclusions

In this work, the effects of solvent and concentration were studied in the absorption and fluorescence spectra of AO. Analysis of four different organic solvents found:

- The intensity and wavelength of the peak of the absorption spectra of acridine dye depend on the type of solvent used.
- There is a red shift of around 5 nm in the maximum wavelength for DMSO, while it remained constant in the other solvents under study.
- The fluorescence spectra of acridine dye solutions shift towards the long wavelength (red shift) with increased concentration.
- The observed results of the fluorescence intensity of AO change significantly due to dye aggregation and strong intermolecular Van der Waals-like attractive forces between the molecules.
- Oscillator strength is less than 1, so the transition is $\pi \rightarrow \pi^*$.
- Stokes shift is highest in water (more polar) and lowest in ethanol (less polar).
- The best value of fluorescence quantum yield in distilled water is around 0.97.
- The fluorescence lifetime was calculated and found that the best value is 13.5 ns in acetone.
- The addition of MgO NPs led to an AO quench in both absorption and fluorescence spectra and an increase in the maximum fluorescence and intensity when Al_2O_3 NPs were added to the solution.

Biographies

Fairooz Faeq Kareem

Department of Physics, College of Science, Mustansiriyah University, Baghdad, Iraq, cenderlla78@yahoo.com, 009647703467140

Mrs Kareem is an Iraqi PhD student in the Department of Physics, College of Science, Mustansiriyah University. She obtained her MSc in Material Physics-Polymers at Mansoura University, Egypt in 2015. She participated in the Sixth International Scientific Conference on Optical Spectrums at the National Research Centre in Cairo in 2015. She participated in a course to develop the capabilities and skills of education staff in Baghdad. She also participated in a workshop to change the physics curriculum textbook at the intermediate stage.

Mahasin F. Hadi Al-Kadhemy

Department of Physics, College of Science, Mustansiriyah University, Baghdad, Iraq, dr.mahasin@uomustansiriyah.edu.iq, 009647705303964

Dr Al- Kadhemy is an Iraqi professor at Mustansiriyah University. She specialises in Material Physics. She has supervised several postgraduate students and published more than 80 articles in global, regional and local journals, some of which are Scopus and Clarivate indexed in the fields of Material Physics, Ceramic Materials, Polymer and Laser dyes, Spectroscopy and Molecular Physics. She has participated in several local and regional seminars, workshops and conferences.

Asrar Abdulmunem Saeed

Department of Physics, College of Science, Mustansiriyah University, Baghdad, Iraq, dr.asrar@uomustansiriyah.edu.iq, 009647901827609

Dr Saeed is an Iraqi assistant professor. She specialises in Material Physics and has supervised several postgraduate master's and doctoral students and published more than 30 articles in global, regional and local journals, some of which are included in Scopus and Clarivate indexes in the fields of Material Physics, Polymer and Laser dyes, Spectroscopy and Molecular Physics. She has participated in several local and regional seminars, workshops and conferences.

ORCID: 0000-00034677-7598

References

Al Hussainey, A.M., Mahmoud, R.K. and Ashrafi, T.M. (2018). Study the optical and spectral properties of the acridine dye as an effective medium in dye lasers. *Journal of University of Babylon for Pure and Applied Sciences*, **26**(10), 167–75.

Albani, J.R. (2007). *Principles and Applications of Fluorescence Spectroscopy*. The UK: Blackwell Publishing Company. DOI: 10.1002/9780470692059.

Al-Kadhemy, M.F. and Nasser, A.A. (2018). Investigation fluorescence energy transfer between two laser dyes: Coumarin 102 and Rhodamine B dissolved in chloroform solvent. *Journal of College of Education*, **1**(3), 141–58.

AL-Kadhemy, M.F., Abbas, K.N. and Abdalmuhadi, W.B. (2020). Physical properties of Rh6G laser dye combined in polyvinyl alcohol films as heat sensor. *IOP Conference Series: Materials Science and Engineering* **928**(7), 072126. DOI: 10.1088/1757-899X/928/7/072126.

Birks, J.B. (1973). Photophysics of Aromatic Molecules. *Wiley Interscience*, **74**(12), 1294–5. DOI: 10.1002/bbpc.19700741223.

Byvaltsev, V.A., Bardonova, L.A. and Onaka, N.R. (2019). Acridine orange: A review of novel applications for surgical cancer imaging and therapy. *Frontiers in Oncology* **9**(925), 1–8. DOI: 10.3389/fonc.2019.00925.

Dihingia, S., Bora, D., Singha, R. and Saikia, P. (2019). Comparative study of oscillator strengths in dye and metal doped silica glasses. *Journal of Physics: Conference Series,* **1330(**1), 1–6. DOI: 10.1088/1742-6596/1330/1/012019.

Falcone, R.D., Correa, N.M. Biasutti, M.A. and Silber, J.J. (2002). Acid-base and aggregation processes of acridine orange base in n-

Heptane/AOT/water reverse micelles. *Langmuir*, **18**(6), 2039–47. DOI: 10.1021/la011411b.

Falcone, R.D., Correa, N.M., Biasutti, M.A. and Silber, J.J. (2006). The use of acridine orange base (AOB) as molecular probe to characterize nonaqueous AOT reverse micelles. *Journal of Colloid and Interface Science*, **296**(1), 356–64. DOI: 10.1016/j.jcis.2005.08.049.

Hotta, K., Yamaguchi, A. and Teramae, N. (2010). Properties of a metal clad waveguide sensor based on a nano porous-metal-oxide/metal multilayer film. *Analytical Chemistry*, **82**(14), 6066–73. DOI: 10.1021/ac100654b.

Kowalewska, M.G., Cholewiński, G. and Dzierzbicka, K. (2017). Recent developments in the synthesis and biological activity of acridine/acridone analogues. *The Royal Society of Chemistry,* **7**(26), 15776–804. DOI: 10.1039/c7ra01026e.

Krolenko, S.A., Adamyan, S.Ya., Belyaeva, T.N. and Mozhenok, T.P. (2006). Acridine orange accumulation in acid organelles of normal and vacuolated frog skeletal muscle fibres. *Cell Biology International*, **30**(11), 933–9. DOI: 10.1016/j.cellbi.2006.06.017.

Kumar, V., Ayushi, J., Shweta, W. and Surinder, K.M. (2018). Synthesis of biosurfactant-coated magnesium oxide nanoparticles for methylene blue removal and selective Pb^{+2} sensing. *IET Nanobiotechnology*, **12**(3), 241–53. DOI: 10.1049/iet-nbt.2017.0118.

Lewkowics, J. (2006). *Principles of Fluorescence Spectroscopy*. 3rd edition. Switzerland: Springer Nature.

Lide, D.R. (2010). *CRC Handbook of Chemistry and Physics*. London: Taylor and Francis Group LLC.

Markarian, S.A. and Gohar, A.S. (2015). The effect of dimethylsulfoxide on absorption and fluorescence spectra of aqueous solutions of acridine orange base. *Spectrochimica Acta - Part A: Molecular and Biomolecular Spectroscopy,* **151**(n/a), 662–6. DOI: 10.1016/j.saa.2015.06.126.

Musarat, A., AlMusayeiba, N.M., Alarfaj,N.A., El-Tohamy,M.F. and Oraby, H.F. (2020). Biogenic green synthesis of MgO nanoparticles using *Saussurea costus* biomasses for a comprehensive detection of their antimicrobial, cytotoxicity against MCF-7 breast cancer and Photocatalysis Potentials. *PLoS ONE,* **15**(8), 1–23. DOI: 10.1371/journal.pone.0237567.

Robinson, B.H., Loffler, A. and Schwarz, G. (1972). Thermodynamic behaviour of acridine orange in solution. *Journal of the Chemical Society*, **69**(1), 56–69.

Saeed, A.A., Kadhum, F.J., Abbas, K.N., Al-Kadhemy, M.F. and Neamah, Z.J. (2020). Effects of anthracene doping ratio and UV irradiation time on photo-fries rearrangement of polycarbonate. *Baghdad Science Journal*, **17**(2), 652–62. DOI: 10.21123/bsj.2020.17.2(SI).0652.

Sharma, V.K., Sahare., P.D., Rastogi, R.C., Ghoshal, S.K. and Mohan, D. (2003). Excited state characteristics of acridine dyes: Acriflavine and acridine orange. *pectrochimica Acta - Part A: Molecular and Biomolecular Spectroscopy*, **59**(8), 1799–804. DOI: 10.1016/S1386-1425(02)00440-7.

Sikiru A.A., Nelson, O.O., Bamgbose, J.T. and Abideen I.A. (2016). Solvent enhancement of electronic intensity in acridine and 9-aminoacridine. *Journal of Saudi Chemical Society* **20**(1), S286–92. DOI: 10.1016/j.jscs.2012.11.002.

Sunandan, P., Swayamprava, D., Prathna, T.C., Shruti, T., Radhika. M., Ashok, M.R., Chandrasekaran, N. and Amitava, M. (2013). Cytotoxicity of aluminium oxide nanoparticles towards fresh water algal isolate at low exposure concentrations. *Aquatic Toxicology* 132–133(n/a), 34–45. DOI: 10.1016/j.aquatox.2013.01.018.

Takashi, K., Fujii, K. and Sakoda, K. (2010). Ultrafast energy transfer in a multichromophoric layered silicate. *Physics and Materials Chemistry*, **114**(2), 983–9. DOI: 10.1021/jp910341f.

Valeur, B. (2012). *Molecular Fluorescence Principles and Application*. 2nd edition. Weinheim: Wiley-VCH Verlag GmbH.